

Kinetics and Parameters of Epitaxial Monolayered Continuous large area Molybdenum disulfide Growth

Rakesh K. Prasad¹, Dilip K. Singh^{1*}

¹ Birla Institute of Technology Mesra, Ranchi -835215 (India)

*Email: dilipsinghnano1@gmail.com

Abstract

The growth of large crystallite continuous monolayer materials like molybdenum disulfide (MoS₂) with desired morphology via chemical vapor deposition (CVD) remains a challenge. In CVD, the complex interplay of various factors like growth temperature, precursors, and nature of the substrate decides the crystallinity, crystallite size, and coverage area of the grown MoS₂ monolayer. In the present work, we report about the role of weight fraction of molybdenum trioxide (MoO₃), Sulfur, and carrier gas flow rate towards nucleation and monolayer growth. The concentration of MoO₃ weight fraction has been found to govern the self-seeding process and decides the density of nucleation sites affecting morphology and coverage area. Carrier gas flow of 100 sccm argon results into large crystallite continuous films with lower coverage area (70 %), while the flow rate of 150 sccm results into 92 % coverage area with reduced crystallite size. Through systematic variation of experimental parameters, we have established the recipe for the growth of large crystallite atomically thin MoS₂ suitable for optoelectronic devices.

Keywords: 2D Materials, Molybdenum disulfide, amount of precursors, gas flow rate, monolayer, continuous growth

Introduction

For past nearly a decade, two-dimensional (2D) semiconducting transition metal dichalcogenides (TMDs), MX_2 ($\text{M}=\text{Mo}, \text{W}$; $\text{X}=\text{S}, \text{Se}$) have attracted huge attention due to their distinct structural, physical, and chemical properties arising from the layered structure with Van der Waal forces of interaction in between the layers opening up new possibilities in the form of efficient and thin electronic and optoelectronic devices. [1-3]. Molybdenum disulfide (MoS_2) is a layered 2D semiconducting material with bandgap in the range 1.2 eV to 1.9 eV, whose optical and electrical properties are dependent on the number of layers [4]. Monolayered MoS_2 is an atomically thin direct bandgap semiconductor with considerable enhancement in the photoluminescence, while increase in the number of layers shows indirect bandgap semiconducting behavior [5]. Monolayered MoS_2 have high potential application in the domain of optoelectronics, nano-electronics and photonics[1,4].

A number of techniques have been attempted to achieve large crystals of single-layered MoS_2 . Initially, various types of exfoliation techniques were explored like scotch tape-assisted micromechanical exfoliation [6], liquid-phase exfoliation [7], electrochemical Li-intercalation from bulk natural crystals [8]. These methods allowed to achieve nanometer to few micrometer sizes of monolayered MoS_2 . To grow films at desired locations with the predefined number of layers having large coverage area, different growth techniques were attempted like thermolysis of ammonium thiomolybdate [9], physical vapor deposition (PVD) [10], atomic layer deposition (ALD)[11,12], hydrothermal synthesis [13], sulfurization of molybdenum[14-16] or molybdenum oxide film[17] and chemical vapor deposition (CVD) [14]. CVD-based growth has the potential to be integrated with in-line fabrication at foundries making it the most favorable

technique used for the synthesis of monolayered MoS₂ having large crystallite size and continuity over a large area.

To elucidate the growth mechanism of MoS₂ films using CVD, recently a number of experiments has been reported. One of the earlier attempts in 2012 used pre-deposited Mo film followed by CVD based sulphurization to achieve single and few-layered MoS₂ on Si/SiO₂ substrate [14]. In 2014 using atmospheric pressure CVD and precursors in the form of sulfur and MoO₃ powders, S.Wang et al. demonstrated that the local change of Mo:S precursors ratio govern the variation of the shapes of the crystals grown from triangular to hexagon [18]. Growth of MoS₂ films using MoO₃ as precursor shows triangular crystals while MoCl₅ based growth results into continuous growth [19]. Single crystalline MoS₂ flakes with size larger than 300 μm was grown by suppressing the nuclei density thorough adjusting the distance between sources and the substrate [20]. Single step synthesis of monolayered large area MoS₂ films were grown on variety of substrates by using the naturally formed gap between SiO₂ coated wafer and the substrate acting as reactor cavity[21]. In another experiment, MoO₂ was used as a precursor and growth kinetics of MoS₂ was elucidated. They observed formation of two types of seeding centers: (a) Mo-oxysulfide (MoO_xS_{2-y}, y<x) nanoparticles resulting into triangular growth for few layers MoS₂ and (b) atomic scale MoS₂ monolayer clusters to grow monolayer and irregular polygon shape [22]. Zhe et al. observed that the monolayered MoS₂ grown from irregular polygonal shaped cluster decorated with S-Mo and Mo-zz edges in a comparable ratio with dominant Mo-zz edges formation grows. Reactant concentration has been found to facilitate 2D-planar nucleation mechanism responsible for monolayer/bi-layer growth while, higher concentration leads to self-seeding nucleation mechanism responsible for few-layered / multi-layered growth [23]. A comparison of growth quality using three different precursors namely

MoO₃, ammonium heptamolybdate (AHM), and tellurium (Te) assistance using MoO₃ for large continuous films using CVD shows better quality of large size growth using only MoO₃ powder and Sulfur powder with a particular ratio of approx. 30:1 [24]. Growth at varying temperature shows that MoS₂ tend to grow laterally in triangular shapes a temperature below 730 °C, while growth above 730 °C results into longitudinal growth with hexagonal shapes [25]. In spite of number of notable attempts, a standard recipe for the growth of continuous large crystallites of MoS₂ remains as a challenge [26,27]. A proper understanding of the growth mechanism is desirable for the CVD-based process to achieve large crystallite continuous monolayered film of MoS₂ having fewer grain boundaries which limits the mobility of the charge carriers [28]. During CVD based growth of MoS₂ number of parameters like nature of the precursor used [29,30] orientation of the substrate [31], gas flow rate [23], growth temperature & duration [25], and use of promoters [32] are expected to affect the crystallite size, phase, and shape.

In this work, MoS₂ grown at various experimental conditions has been systematically investigated using spectroscopic tools to establish the recipe for growth of continuous monolayered MoS₂ film having limited grain boundaries. The role of grain boundaries formation and triangular domains has been elucidated to achieve large area MoS₂ atomically thin films for electronic and opto-electronic applications.

Experimental setup

For MoS₂ growth highly pure molybdenum trioxide MoO₃ (99.9 % sigma Aldrich) and sulfur powder (99.9% Sigma Aldrich) were used as precursors. Figure 1(a) shows the schematic of the CVD setup and parameters of MoS₂ growth are shown in Fig. 1(b)-(c). In CVD, the quartz tube

of length 120 cm and diameter 4.5 cm was used. Temperature profile of both the precursors (MoO_3 and S powder) during complete cycle of growth has been shown in Fig. 1(b) and gas flow rate for the complete experimental duration. 285 nm SiO_2/Si wafer was used as a substrate for growth. The substrate was first cleaned sequentially using the iso-propyl alcohol, water and ethanol through the sonication bath process for 15 min each. After sonication, the substrate was washed with deionized water and then dried using the argon gas and put inside the hot oven at 100 °C for 10 min. The polished surface of the substrate faces downward to the precursor above the MoO_3 powder. Precursors and substrate were placed inside the CVD furnace as schematically shown in Fig. 1(a) separated at 19 cm. The growth was carried out at 750 °C for 5 mins using a single zone CVD furnace at atmospheric pressure. The outlet of the quartz tube was bubbled through a water bucket ensuring an equilibrium argon pressure inside the tube. During growth the amount of MoO_3 was varied between 10 mg to 30 mg referred as SET-I keeping gas flow rate constant 100 sccm and weight of sulfur 200 mg. In SET-II, the weight of the second precursor sulfur was varied in the range 100 mg to 500 mg keeping other conditions like weight of MoO_3 (15 mg) and gas flow rate (100 sccm) fixed. Finally, the carrier gas flow rate (Argon) was varied in the range 50 sccm to 300 sccm referred as SET-III, while keeping the other two factors MoO_3 and sulfur fixed at 15 mg and 200 mg respectively.

Characterization

The growth of MoS_2 flakes were confirmed initially using an optical microscope (Leica) with 10× (NA 1.3), 50× was used for optical micrograph. The detailed morphology of grown samples was recorded using a field emission electron microscope (ZEISS Sigma 300 FESEM). The number of layers of MoS_2 was characterized using a Raman spectrometer (Renishaw Invia-

Raman Spectrometer) in the range 350-450 nm. The photoluminescence spectra of samples were recorded in the range 500-800 nm using $\lambda_{ex}= 514$ nm (laser excitation).

Result and discussion

Figure 2(a) shows the optical microscope image of the grown continuous film of MoS₂ sample. FESEM image of individual triangle at higher magnification grown continuous sheet of MoS₂ film is shown in Fig. 2 (b). Raman spectra shows two vibration modes at 385.7 (E'_{2g}) and 405 cm^{-1} (A_{1g}) as shown in figure 2(c). Observed frequency difference of 19.5 cm^{-1} confirms growth of monolayer MoS₂ in agreement with previous work [14,24] . The frequency difference between these two modes depends upon the number of layers [33]. Both the in plane vibrational mode (E'_{2g}) and out of plane (A_{1g}) modes shows requirement of two-peak structure for fitting the experimental curve as shown in Fig.2 (c). Fitted line profile is summarized in Table-I. Interestingly, the in-plane vibrational mode (E'_{2g}) mode is Gaussian while out of plane (A_{1g}) mode is Lorentzian in line-shape. Such two peak structure / splitting of in plane vibrational mode (E'_{2g}) was previously observed in MoS₂ with lattice strain of more than 1 %, which arises due to disorder in the crystalline structure of the material [34].The photoluminescence spectra recorded from same position is shown in Fig. 2(d). The experimental curve was fitted using Gaussian line shape which shows emission peak at 679.2 nm (1.83 eV) with shoulders at 624.4 nm (1.99 eV) with relative intensities of 4421 counts and 1869 counts respectively. The 1.83 eV peak is assigned to the A-exciton while 1.99 eV peak arises due to B-excitons [35,36]. A-exciton shows peak width $\Delta\omega = 44.1$ nm, while the B-exciton shows $\Delta\omega = 63.7$ nm. Observed strong A-exciton peak relative to the B-exciton indicates monolayer growth [5] in agreement with the Raman spectra shown previously. R. Coehoorn et al. observed two prominent peaks at 670 and 627 nm

in the absorption spectrum. These two resonances have been established to be the direct excitonic transitions at the Brillouin zone K point. Their energy difference is due to the spin-orbital splitting of the valence band. [35,36].

Fig. 3 shows the effect of MoO₃ weight fraction during growth. Fig. 3(a) shows nucleation of small equilateral triangular domains randomly on the substrate having crystallite size ~7 μm when 10 mg of MoO₃ was used along with 200 mg of sulfur. Lower concentration of MoO₃ results in a lower growth rate. Optical image of growth with 15 mg MoO₃ indicates formation of continuous films with large crystal size ~ 30 μm. Increased MoO_{3-x} vapor flux with increasing weight fraction of MoO₃ leads to increased growth rate resulting into formation of continuous films with grain boundaries as visible in Fig. 3(b). Grain boundaries of continuous film formation were observed due to low mass flux and high growth rate [37], Coalescence of the particles takes place resulting into formation of continuous sheet with increased MoO₃ weight fraction to minimize the surface energy through reduction of surface area. With further increase of MoO₃ concentration to 20 mg, multi-nucleation sites were observed under optical microscope as shown in Fig. 3(c). In this case we observe continuous film with discrete crystal size range from ~7 to 25 μm (Fig. 3(c)). For 25 mg of MoO₃, the crystal shape changes from sharp edged triangles to triangles with rounded corners having crystallite size of 7 μm as shown in Fig 3(d). Further increase of MoO₃ weight fraction to 30 mg results into triangular crystals with smaller size ~7 μm and higher nucleation density on the substrates as shown Fig. 3(e). Growth with increasing weight of MoO₃ relative to sulfur results into large crystal of MoS₂ flakes with continuous films tuned by Vapor phase of MoO_{3-x}. The precursor evaporates in the form of flux, resulting into different size nanostructures. The deposition of MoO_{3-x} molecular clusters are reduced to MoS_{2-x} clusters (bright spots inside the triangle) in the initial stage of the growth

process, consequently leading to a 2-dimensional nucleation on SiO₂/Si substrate (as shown schematically in figure S1 ó Supplementary information)[38]. The growth of MoS₂ is limited by the diffusion of vapor-phase MoO_{3-x} [39]. Tuning of weight fraction of precursor also affects Mo:S molar ratio along the substrate which affects the morphology of MoS₂, on the basic principle of crystal growth [18]. As we increase the amount of MoO₃ to 15 mg, the density of MoO_{3-x} clusters increases gradually with a proper ratio 1:60 of Mo:S atom concentration which forms a continuous film of MoS₂ flakes. Higher concentration of MoO₃ leads to multiple MoS_{2-x} clusters resulting into formation of multilayer growth. 30 mg MoO₃ precursor leads to formation of multiple bright spots due to incomplete sulfurization of number of clusters [22,23]. With increasing MoO₃ weight fraction the coverage area monotonically increases while the variation in domain size shows a maximum at 15 mg of MoO₃ as shown graphically in fig. 3(f). (Figure.S1- Supplementary information) schematically shows the variation of the nucleation centers density with increasing MoO₃ concentration. Interestingly, even in the past experiments, 15 mg of MoO₃ has been found to result into continuous sheet of MoS₂ [18,21] and the concentration of Mo governs the shape and size of Monolayer MoS₂ crystals [40].

To understand the change in the crystal structure and to quantify the number of layers, samples of SET-1 were subjected to Raman spectroscopy measurements. Spectra were collected from different regions of the sample as shown in Fig. 4(a). Raman spectra shows two prominent peaks at ~ 384 cm⁻¹ and ~ 406 cm⁻¹ assigned to in-plane $\Gamma_{2\mu}^{\Gamma}$ vibration mode and out of plane $\Gamma_{2\mu}^{\Gamma}$ vibration mode. In plane E_{2g}¹ vibration mode arises due to in plane vibration of Mo and S atoms, while out of plane $\Gamma_{2\mu}^{\Gamma}$ vibration mode arises due to out of plane vibration of Sulphur atoms [33]. The peak width of these modes was estimated upon fitting E_{2g}¹ and A_{1g} modes with Gaussian and Lorentzian line-shape respectively as summarized in Table-I (fitted curves shown

in Supplementary information Figure S2). Lorentzian line shape indicates high crystallinity of as grown MoS₂ films. The difference in the peak position of Γ_{22}^{\prime} and $\Gamma_{22}^{\prime\prime}$ modes indicates the number of layers due to weak van der waals interlayer coupling, and the presence of coulombic interlayer interaction in MoS₂ [33]. E_{2g}^{\prime} and A_{1g} modes are shifted as additional layers added to form the bulk material from individual layer because interlayer van-der wall interaction increase the effective restoring force acting on the atoms [41]. With decreasing number of layers A_{1g} mode shifts closer to E_{2g}^{\prime} modes [33]. Sample grown with 10, 20, 25 and 30 mg shows peak separation of 25.2 cm⁻¹, 23.8 cm⁻¹, 19.8 cm⁻¹ and 22.6 cm⁻¹. Raman spectra of samples grown with 25 mg of MoO₃ indicated monolayered growth. While growth with 30 mg of MoO₃ indicates bilayer growth as evident. The higher relative concentration of MoO₃ as compared to sulfur leads to initialization of multi-nucleation sites resulting into multilayer growth, while growth with 25 mg of MoO₃ results into monolayered growth. In the case of layered growth the deposit MoO₃ wets the substrate due to dominance of surface tension between substrate-vapor (γ_{sv}) over combined effect of surface tension between film-substrate (γ_{fs}) and film-vapor (γ_{fv}) i.e. $\gamma_{sv} \geq \gamma_{fs} + \gamma_{fv}$. [38] Fig. 4(b) shows the photoluminescence spectra of samples. The spectral line profile was obtained by fitting with the gaussian lineshape as summarized in Table-II (fitted curves shown in Supplementary information Figure S3). Grown sample with 10 mg of MoO₃ shows peaks at ~ 671 nm (1.85 eV) and 628.6 nm (1.97 eV) corresponding to A-exciton and B-exciton respectively. Fitting of PL spectra requires two Gaussian peaks for A-exciton in addition to B-peak at ~ 671.4 nm (1.85 eV) and 681.3 nm (1.82 eV) respectively. A and B exciton arises due to spin-orbit coupling induced splitting of valence band [5]. MoO₃-10 shows a relatively weaker luminescence peak, indicating multilayer growth in agreement with the observed Raman spectra. With increase of the MoO₃ weight fraction to 20 mg leads to observation of highest PL

intensity and with further increase the PL intensity monotonically decreases. Strong emission indicates presence of direct band, high crystalline quality of grown monolayer films. With increasing number of layers to bi-layers and tri-layers, the luminescence intensity gets suppressed and disappears [5]. At lower concentration (10 mg) and moderate 15 mg concentration of MoO₃, we observed a planar flake but with higher concentration (20 and 25 mg) the flakes contained nanocrystals on the MoS₂ flakes. At much higher concentration (30 mg) the size decreased with increase in the density of nanocrystals over the MoS₂ flakes. Thus, concentration of MoO₃ is responsible for self-seeding process and their concentration decide the nucleation site and coverage area. At much higher concentration the density of nanocrystals increases indicating incomplete sulphurization. Similar observations has been reported by D. Zhu et al. [22]. Samples grown with 25 mg and 30 mg of MoO₃ shows two peak structures for the direct-gap transition referred as A-exciton peak (i.e. A-exciton peak and A⁻ trions peak) [42]. Previously negative doping of MoS₂ by SiO₂ substrate has been accounted for the origin of A⁻ trion emission and observed red shift with broadened main peak in PL [43]. Interestingly in our experiment, except weight fraction of MoO₃ all other parameters were kept fixed, observation of A⁻ trion in samples grown using higher MoO₃ weight fractions exclusively contradicts the hypothesis proposed previously in terms of substrate induced negative doping effect, since the common substrate was used in all sets of experiments. In another work, observation of A⁻ trions peak has been accounted to high purity interface between the sample and the substrate [20].

Fig. 5 shows growth of MoS₂ with varying amount of sulfur relative to MoO₃ (SET-II), keeping weight of MoO₃ powder fixed at 15 mg and gas flow rate 100 sccm. Fig. 5(a) shows results with 100 mg of sulfur. MoS₂ flakes at random locations on the substrate were formed having shapes varying from triangle to star like pattern with crystallite size of ~11 nm. On

substrate, there is a small triangular growth of MoS₂ flakes due to lower concentration of sulfur in the growth atmosphere near the surface. Doubling the sulfur amount to 200 mg results into crystallite size of ~ 30 μm and continuous film upto few mm² as observed in Fig. 5(b). With further increase of weight fraction to 300 mg of sulfur, MoS₂ crystals with triangular shape and varying crystallite sizes ~ 7 to 25 μm were observed, Fig. 5(c). Also crystallite domains were not continuous as observed at lower weight fractions. If the weight of the sulfur is increased to 400 mg, the crystallite size of the triangular MoS₂ flakes is reduced to ~ 7 μm due to decrease in lower concentration of Mo:S atom ratio, Fig. 5(d). With excessively large weight fraction of sulfur to 500 mg, formation of star like flakes were observed having average crystallite size of about ~ 20 μm (Fig. 5(e)). A closer observation to the center of the star flakes indicates the presence of clusters responsible for multinucleation. Due to the sufficient amount of sulfur, multi-layer formation is observed. Proper weight fraction of sulfur has been observed as the prime factor deciding formation of number of layers/ crystallite size. It's clear from the optical micrographs that a proper amount of Mo:S ratio of the precursor plays critical role towards maintaining triangular shape [44]. With varying concentration of Sulfur, the nucleation density significantly changes in contrast to previous report where the role of sulfur towards nucleation was found to be negligible [20].

Fig. 6 shows optical micrograph of MoS₂ samples grown with varying gas flow rates (50 to 300 sccm) keeping precursors weight MoO₃ (15 mg) and Sulfur (200 mg) constant. Growth with 50 sccm of Argon flow results into MoS₂ flakes having large crystallite size of ~ 80 μm and coverage area of ~ 40 % as shown in Fig. 6(a). With moderate gas flow rates (100 and 150 sccm) the discrete crystals of MoS₂ flakes join together to form continuous films. Gas flow rate of 100 sccm results into coverage area of 70 %, while flow rate of 150 sccm leads to 92 % coverage

area as shown in figure 6(b). Further increase of gas flow rate to 200, 250 and 300 sccm results into smaller crystallites with discrete regions. A gas flow rate of 300 sccm results into MoS₂ crystallites of size as small as ~ 7 nm. It is obvious from the optical micrographs shown in Fig. 6 (c)(d)and(e) respectively that carrier gas flow rate is another key parameter which influence the crystallite size and coverage area by tuning the local concentration of MoO_{3-x} and sulfur vapor precursors being nucleated on the substrate. Carrier gas flow rate decides the residence time of vapors of precursors on the substrate deciding nucleation density, crystallite size and coverage area. Under sufficient supply of precursor and nucleation sites, the growth extends in the form of large-area single-layered MoS₂ continuous film with increasing gas flow rate as shown in figure 6(f). It is also interesting to note that with increase of the crystallite size, the coverage area decreases.

Fig. 7 shows effect of change of molar ratio of Mo and Sulfur on the crystallite size and on the coverage area. The change in the morphology of MoS₂ along the gas flow direction in the Mo: S atom ratio along the Si substrate surface. With increasing molar ratio from 30:1 to 60:1 the crystallite size increases. With further increase of the molar ratio, the crystallite size monotonically decreases for the molar ratios 90:1 and 120:1. Growth using increased molar ratio to 150:1 shows increase in the crystallite size. A molar ratio of 60:1 results into MoS₂ crystals of average size ~30 μm, while molar ratio of 60:1 results into continuous films. MoS₂ crystals grown with molar ratio of 90:1 shows the strongest photoluminescence intensity, indicating monolayer growth. Under all attempted growth conditions by varying precursor's weight fractions, gas flow rates, we obtained triangular shaped MoS₂ growth. While V Senithikumar et al. [45] observed variation in the grown crystallites due to growth under low pressure. It's interesting to observe that the crystallite shape remains triangular due to growth under

atmospheric pressure conditions using single zone furnace without any requirement of vacuum conditions.

Conclusion

Through controlled growth at various experimental parameters, we have been able to successfully grow continuous films of MoS₂ monolayers on SiO₂/Si substrate through CVD. Optimized precursor weight ratio i.e MoO₃ and Sulphur (15 mg: 200 mg) results into discrete crystallite size as large as 80 nm with 50 sccm flow of Argon as carrier gas and coverage area of ~ 40 %. Thus, concentration of MoO₃ is responsible for self-seeding process and their concentration decides the nucleation site and coverage area. With moderate gas flow rates (100 and 150 sccm) the discrete crystals of MoS₂ flakes join together to form continuous films. Gas flow rate of 100 sccm results into continuous film with 70 % coverage area. While flow rate of 150 sccm leads to 92 % coverage area. Increase of the crystallite size leads to decrease in the coverage area. MoO_{3-x} was found to be responsible for self-seeding nucleation and its amount decides the nucleation density. The formation of MoS₂ flakes and its shape is dependent on local concentration which is tuned by the relative amount of MoO₃ and sulfur precursors. The carrier gas flux decides the residence time of Mo and S on the substrate towards growth. The carrier gas flow rate is responsible for local concentration of vapor precursors and their coverage area.

Acknowledgements

One of the authors Rakesh K. Prasad thanks TEQIP-III for fellowship. Dilip K. Singh thanks DST, Government of India (Fellowship IFA13-PH65; CRG/2021/002179; CRG/2021/003705) and Seed Money Scheme, Birla Institute of Technology, Mesra for funding.

Supplementary information

Supplementary information contains schematic diagram of effect of concentration of MoO_3 precursor on self seeding sites along with fitted Raman and photoluminescence spectra plots for MoS_2 flakes grown under different concentration of MoO_3 .

Data availability statement

The datasets generated during and/or analyzed during the current study are available from the corresponding author on reasonable request.

Table I: Fitted parameters of Raman spectra

Sample	Peak-1	Peak-2	Peak-3	Peak-4	Peak-5	Peak-6	
<i>Lineshape</i>			<i>Gaussian</i>			<i>Lorentzian</i>	
<i>Parameters</i>							
MoO ₃ -10	<i>Center</i>		380.2	383.7		408.9	
	<i>FWHM</i>	-	10.1	4.5	-	5.2	
	<i>Ampl.</i>		1044	2299		6424	
MoO ₃ -15	<i>Center</i>		382.1	385.7	405.2	408.9	
	<i>FWHM</i>	-	9.9	3.1	6.5	5.2	
	<i>Ampl.</i>		1118	7125	7280	6424	
MoO ₃ -20	<i>Center</i>	342.3	365.8	380.9	383.8	407.6	409.2
	<i>FWHM</i>	34.1	17.0	10.6	4.5	6.7	4.2
	<i>Ampl.</i>	773	649	1984	3540	9641	4301
MoO ₃ -25	<i>Center</i>	349.3	366.1	382.4	384.8	404.6	
	<i>FWHM</i>	8.3	10.2	10.0	3.4	5.8	-
	<i>Ampl.</i>	220	450	865	4332	2171	
MoO ₃ -30	<i>Center</i>		382.6	384.1	406.7	408.9	
	<i>FWHM</i>	-	11.1	3.0	5.7	3.4	
	<i>Ampl.</i>		2866	16631	10839	11872	
	<i>Assignment</i>		<i>E_{2g}</i>	<i>E_{2g}</i>	<i>A_{1g}</i>	<i>A_{1g}</i>	
	<i>(Lineshape)</i>		<i>Gaussian</i>	<i>Gaussian</i>	<i>Lorentzian</i>	<i>Lorentzian</i>	

Table II: Fitted parameters of PL spectra using Gaussian line-shape

Sample		Peak-1	Peak-2	Peak-3	Peak-4	Peak-5	B/A ratio
	<i>parameters</i>						
MoO ₃ -10	<i>Center</i>	628.6	671.4	-	681.3	-	
	<i>FWHM</i>	39.2	21.5		48.2		
	<i>Ampl.</i>	63	263		244		
MoO ₃ -15	<i>Center</i>	624.4	-	679.2	-	-	
	<i>FWHM</i>	63.7		44.1			
	<i>Amp</i>	1869		4421			
MoO ₃ -20	<i>Center</i>	-	669.8	-	687.5	695.5	
	<i>FWHM</i>		15.77		49.4	132.4	
	<i>Ampl.</i>		1697		7994	2044	
MoO ₃ -25	<i>Center</i>	627.7	670.6	673.5	679.2	-	
	<i>FWHM</i>	38.6	17.1	148.9	42.7		
	<i>Ampl.</i>	722	2796	860	3651		
MoO ₃ -30	<i>Center</i>	627.8	663.9	661.8	677.5		
	<i>FWHM</i>	44.7	16.5	143.2	43.03		
	<i>Ampl.</i>	911	1294	1096	3425		
	<i>Assignment</i>	<i>B-exciton</i>	<i>A-exciton</i>	<i>A⁻-trion</i>			

Figure captions:

Figure-1 (a) Schematic setup for thermal CVD for MoS₂ synthesis (b) Temperature variation for MoO₃ and Sulfur during MoS₂ growth Process. (c) Variation of gas flow rate during growth.

Figure-2 (a) Optical Microscope image of grown MoS₂ flakes (b) FESEM images of MoS₂ grown on 285 nm - SiO₂ /Si (c) Raman Spectra of MoS₂ (d) Photoluminescence spectra from grown MoS₂ films.

Figure-3 Optical micrographs of CVD-grown MoS₂ flakes with varying amounts of MoO₃ precursor (a) 10 mg (b) 15 mg (c) 20 mg (d) 25 mg (e) 30 mg (f) Variation of domain size and coverage area with increasing weight of MoO₃.

Figure-4 (a) Raman spectra of grown MoS₂ with varying MoO₃ weight fraction (b) Photoluminescence spectra.

Figure-5 Optical Microscope images for the CVD-grown MoS₂ flakes with varying amounts of sulfur (a) 100 mg (b) 200 mg (c) 300 mg (d) 400 mg (e) 500 mg, and (f) Dependence of domain size and coverage area on the weight fraction of the sulfur.

Figure-6 Shows the optical image for CVD grown MoS₂ flakes with varying gas flow rate (a) 50 sccm (b) 150 sccm (c) 200 sccm (d) 250 sccm (e) 300 sccm (f) shows dependence of coverage area and crystallite size on carrier gas flow rate.

Figure-7 Effect of molecular ratio (MoO₃: Sulfur) on the (a) Crystallite size and (b) Coverage area %.

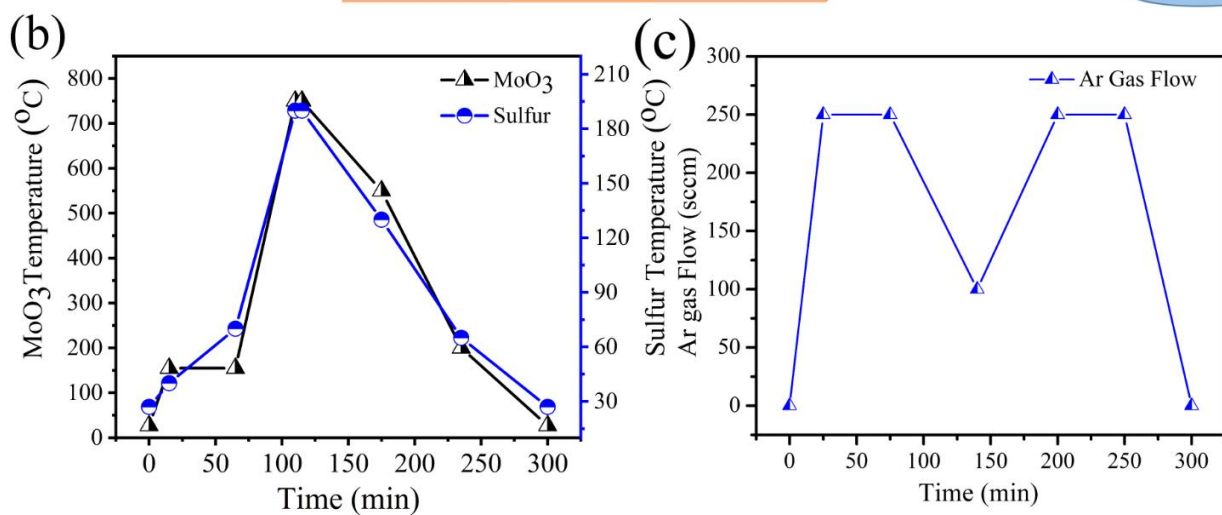
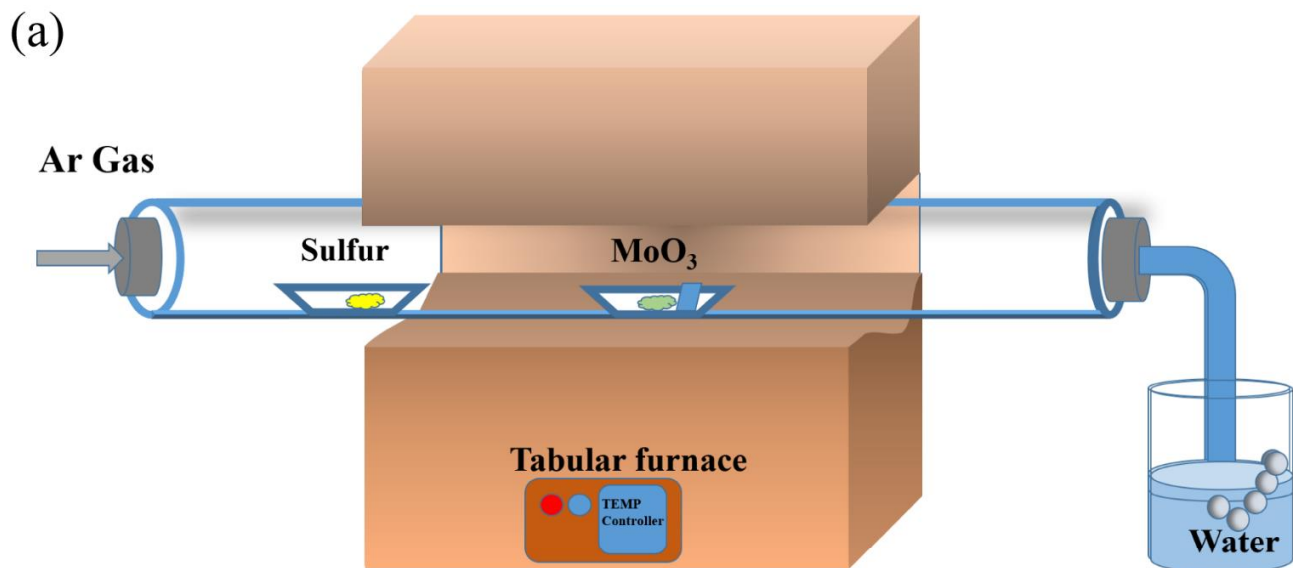


Fig. 1 Singh et al.

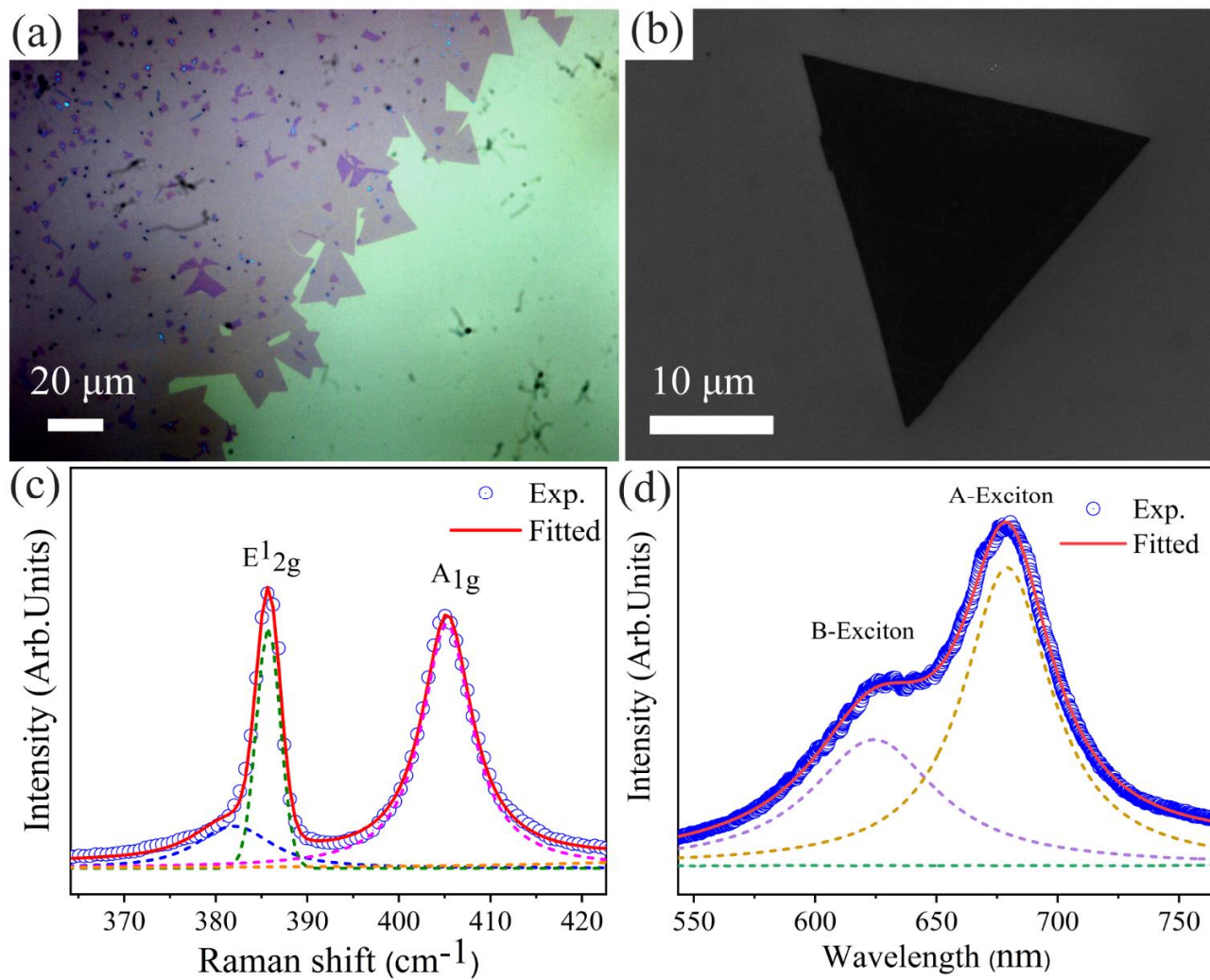


Fig. 2 Singh et al.

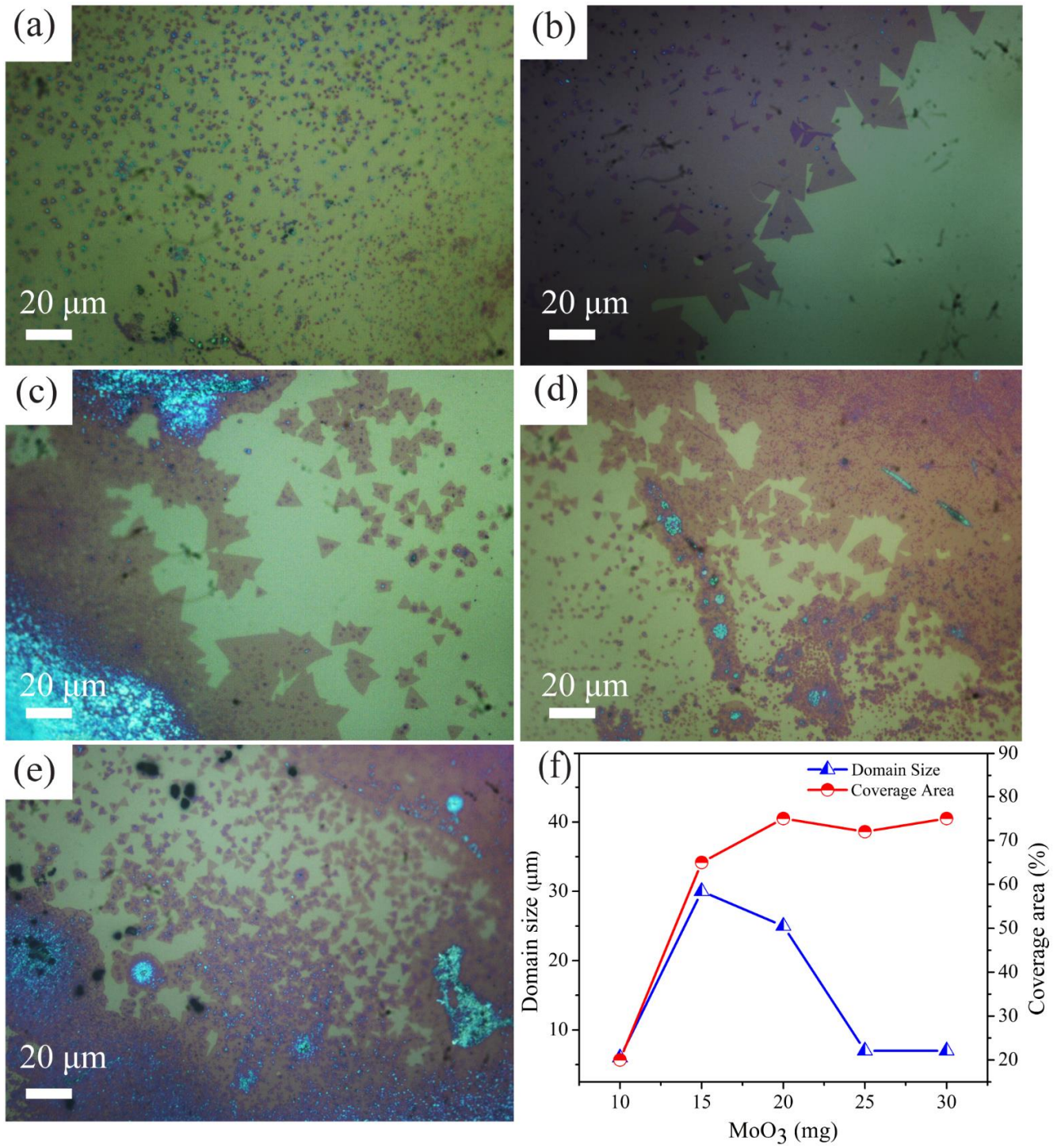


Fig. 3 Singh et al.

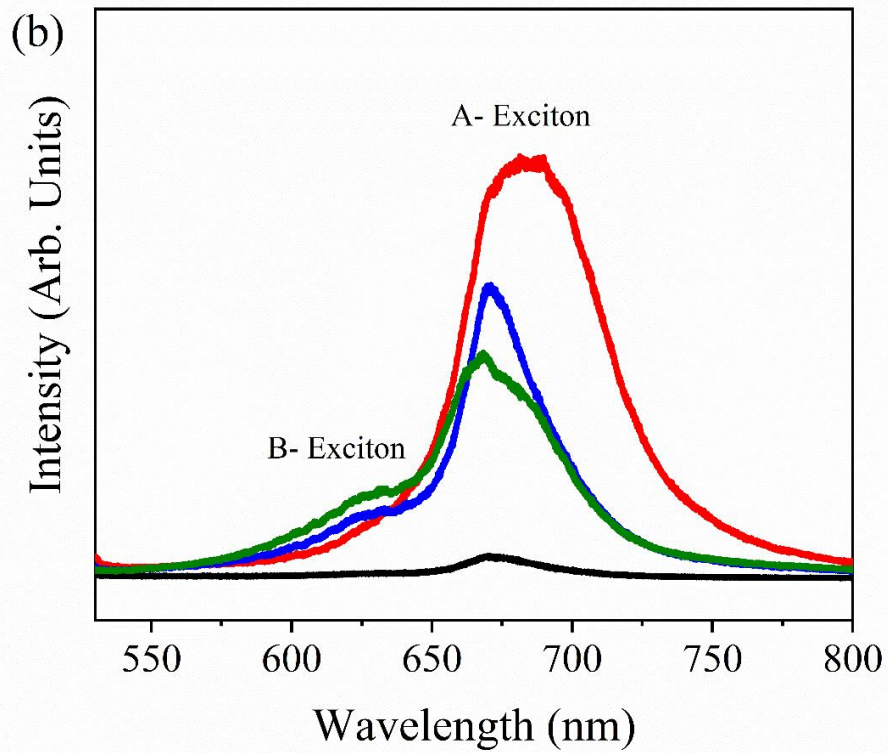
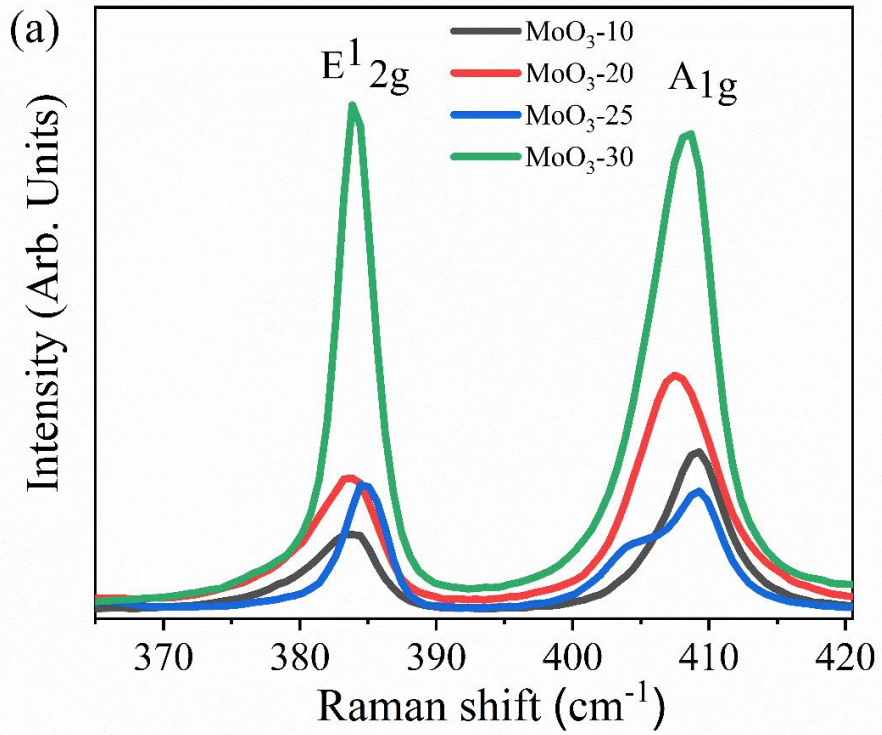


Fig. 4 Singh et al.

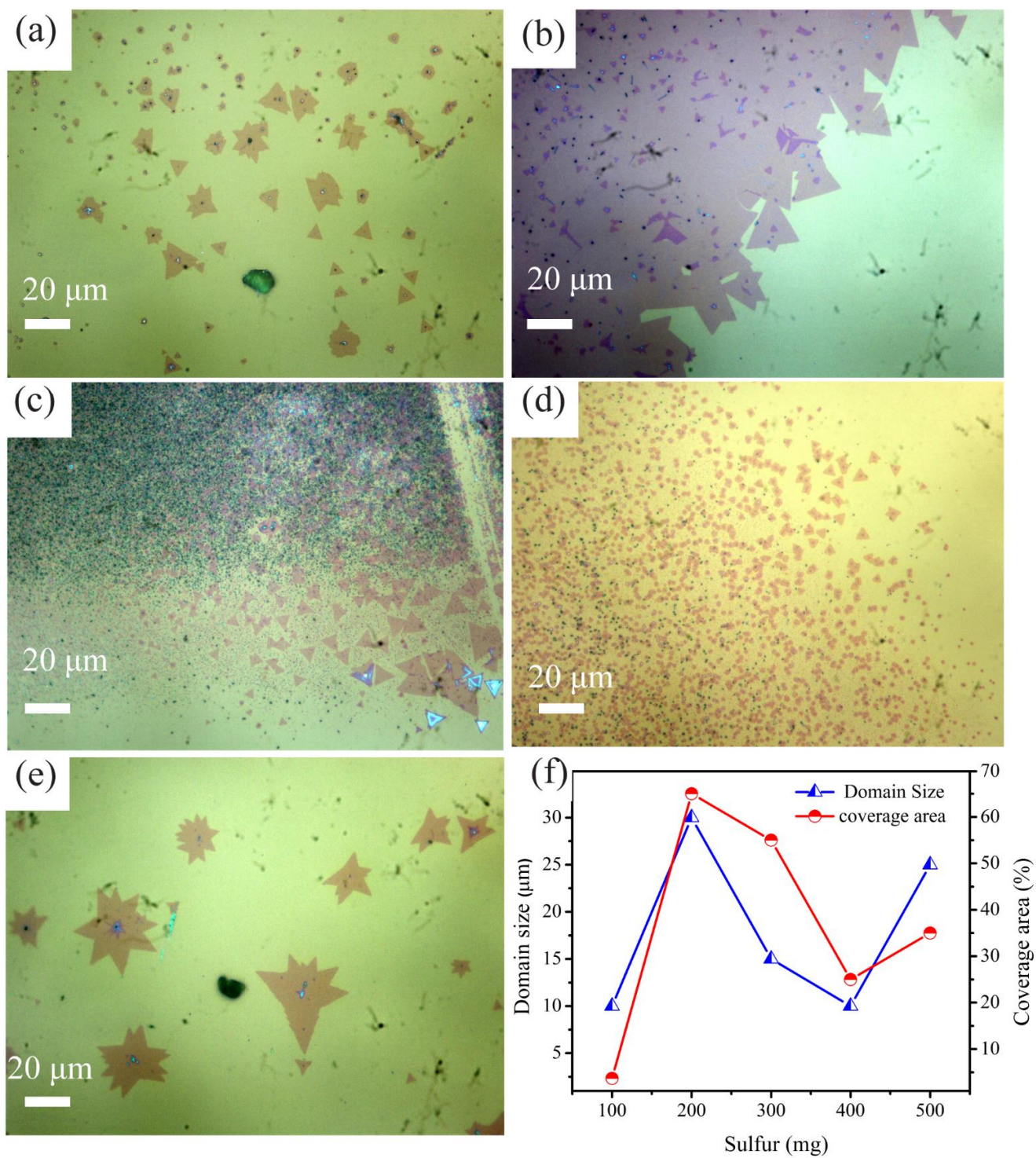


Fig. 5 Singh et al.

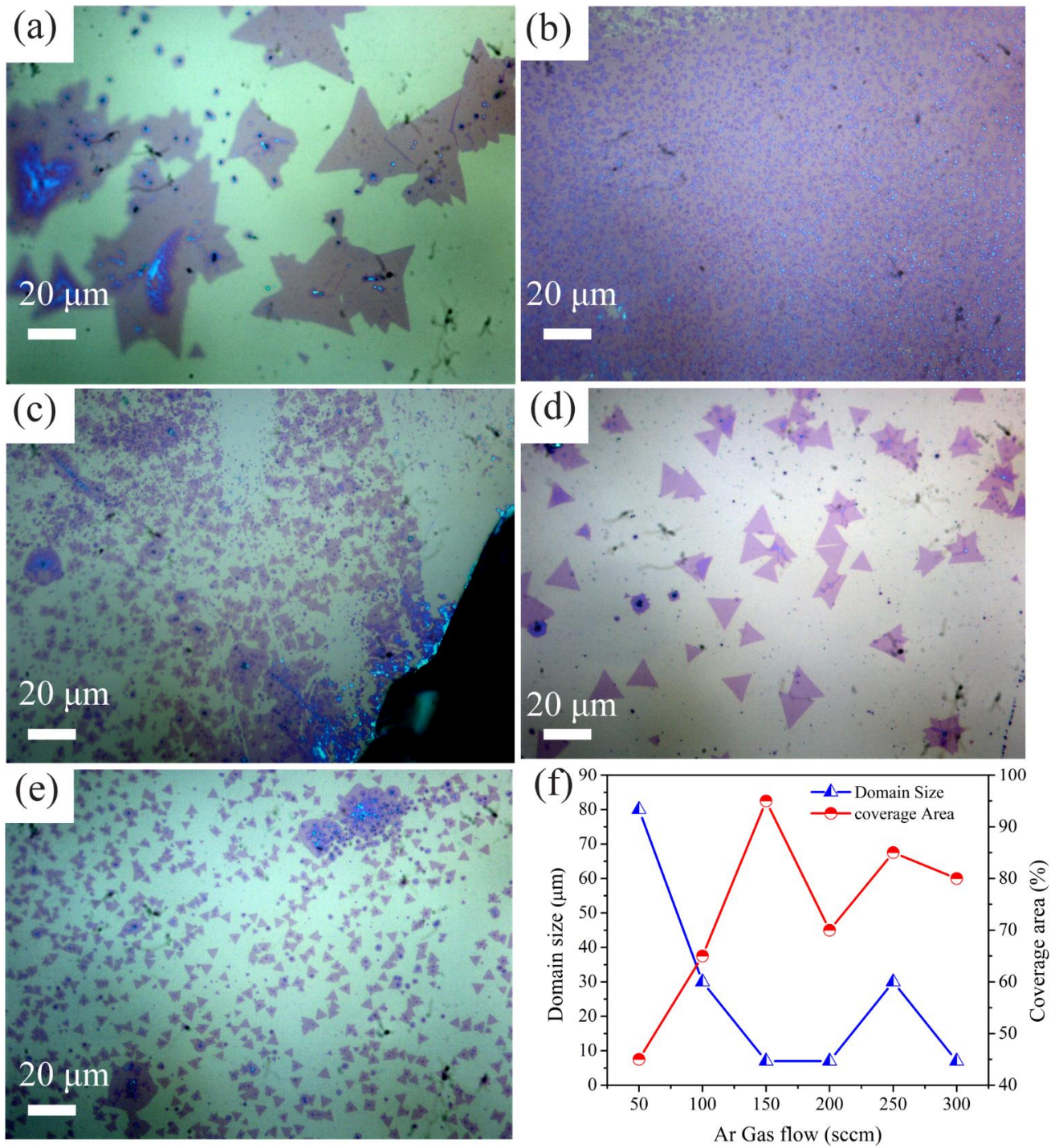


Fig. 6 Singh et al.

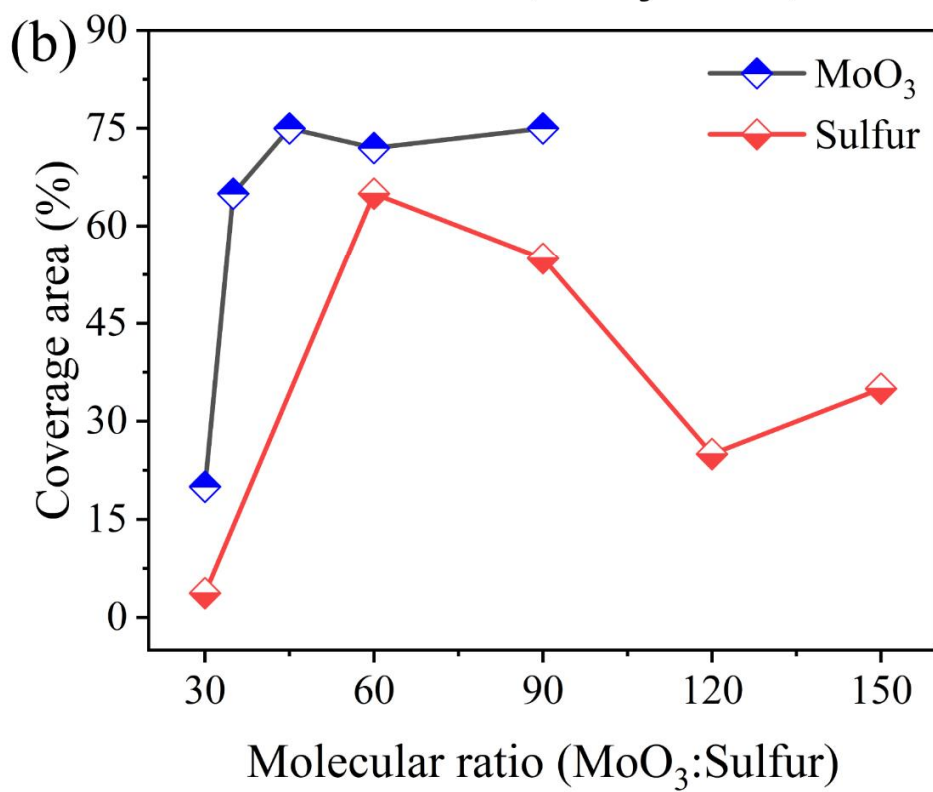
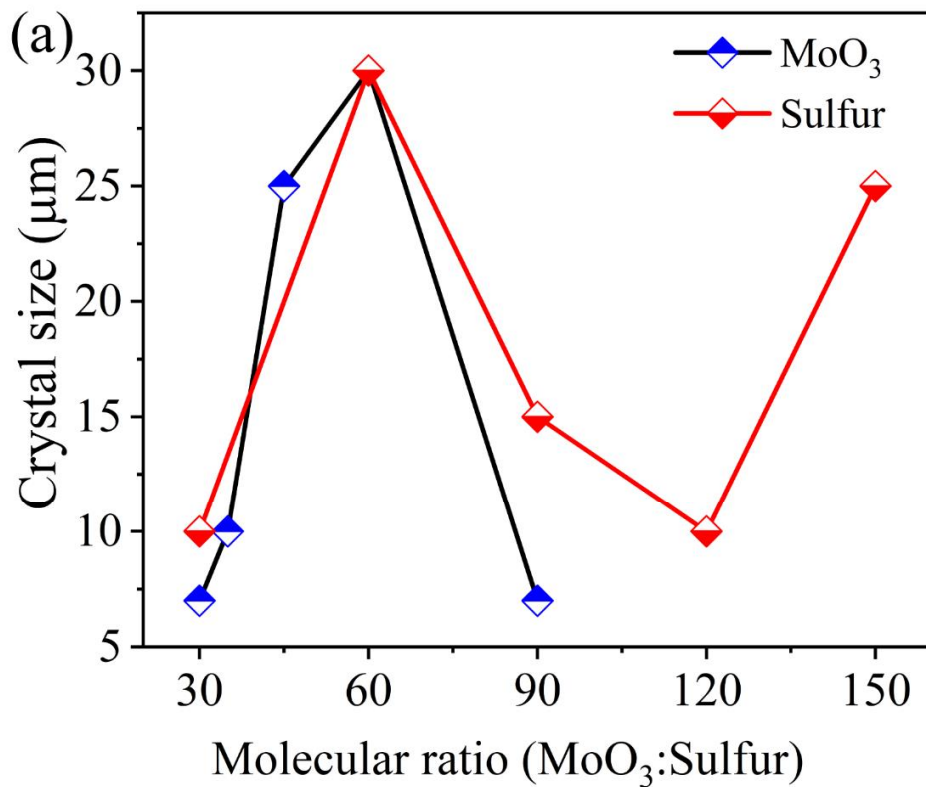


Fig. 7 Singh et al.

References

- [1] Radisavljevic B, Radenovic A, Brivio J, Giacometti V and Kis A 2011 Single-layer MoS₂ transistors *Nature nanotechnology* **6** 147
- [2] Wang Q H, Kalantar-Zadeh K, Kis A, Coleman J N and Strano M S 2012 Electronics and optoelectronics of two-dimensional transition metal dichalcogenides *Nature nanotechnology* **7** 699-712
- [3] Balendhran S, Walia S, Nili H, Ou J Z, Zhuiykov S, Kaner R B, Sriram S, Bhaskaran M and Kalantar-zadeh K 2013 Two-dimensional molybdenum trioxide and dichalcogenides *Advanced Functional Materials* **23** 3952-70
- [4] Mak K F, Lee C, Hone J, Shan J and Heinz T F 2010 Atomically thin MoS₂: a new direct-gap semiconductor *Physical review letters* **105** 136805.
- [5] Splendiani A, Sun L, Zhang Y, Li T, Kim J, Chim C-Y, Galli G and Wang F 2010 Emerging photoluminescence in monolayer MoS₂ *Nano letters* **10** 1271-5
- [6] Novoselov K S, Jiang D, Schedin F, Booth T, Khotkevich V, Morozov S and Geim A K 2005 Two-dimensional atomic crystals *Proceedings of the National Academy of Sciences* **102** 10451-3
- [7] Coleman J N, Lotya M, O'Neill A, Bergin S D, King P J, Khan U, Young K, Gaucher A, De S and Smith R J 2011 Two-dimensional nanosheets produced by liquid exfoliation of layered materials *Science* **331** 568-71
- [8] Zeng Z, Yin Z, Huang X, Li H, He Q, Lu G, Boey F and Zhang H 2011 Single-layer semiconducting nanosheets: high-yield preparation and device fabrication *Angewandte Chemie* **123** 11289-93
- [9] Liu K-K, Zhang W, Lee Y-H, Lin Y-C, Chang M-T, Su C-Y, Chang C-S, Li H, Shi Y and Zhang H 2012 Growth of large-area and highly crystalline MoS₂ thin layers on insulating substrates *Nano letters* **12** 1538-44
- [10] Gong C, Huang C, Miller J, Cheng L, Hao Y, Cobden D, Kim J, Ruoff R S, Wallace R M and Cho K 2013 Metal contacts on physical vapor deposited monolayer MoS₂ *ACS nano* **7** 11350-7
- [11] Tan L K, Liu B, Teng J H, Guo S, Low H Y and Loh K P 2014 Atomic layer deposition of a MoS₂ film *Nanoscale* **6** 10584-8
- [12] Jin Z, Shin S, Han S-J and Min Y-S 2014 Novel chemical route for atomic layer deposition of MoS₂ thin film on SiO₂/Si substrate *Nanoscale* **6** 14453-8
- [13] Rao C and Nag A 2010 Inorganic analogues of graphene *European Journal of Inorganic Chemistry* **2010** 4244-50

- [14] Zhan Y, Liu Z, Najmaei S, Ajayan P M and Lou J 2012 Large-area vapor-phase growth and characterization of MoS₂ atomic layers on a SiO₂ substrate *small* **8** 966-71
- [15] Lee Y, Lee J, Bark H, Oh I-K, Ryu G H, Lee Z, Kim H, Cho J H, Ahn J-H and Lee C 2014 Synthesis of wafer-scale uniform molybdenum disulfide films with control over the layer number using a gas phase sulfur precursor *Nanoscale* **6** 2821-6
- [16] Choudhary N, Park J, Hwang J Y and Choi W 2014 Growth of large-scale and thickness-modulated MoS₂ nanosheets *ACS applied materials & interfaces* **6** 21215-22
- [17] Lin Y-C, Zhang W, Huang J-K, Liu K-K, Lee Y-H, Liang C-T, Chu C-W and Li L-J 2012 Wafer-scale MoS₂ thin layers prepared by MoO₃ sulfurization *Nanoscale* **4** 6637-41
- [18] Wang S, Rong Y, Fan Y, Pacios M, Bhaskaran H, He K and Warner J H 2014 Shape evolution of monolayer MoS₂ crystals grown by chemical vapor deposition *Chemistry of Materials* **26** 6371-9
- [19] Ganorkar S, Kim J, Kim Y-H and Kim S-I 2015 Effect of precursor on growth and morphology of MoS₂ monolayer and multilayer *Journal of Physics and Chemistry of Solids* **87** 32-7
- [20] Lin Z, Zhao Y, Zhou C, Zhong R, Wang X, Tsang Y H and Chai Y 2015 Controllable growth of large-size crystalline MoS₂ and resist-free transfer assisted with a Cu thin film *Scientific reports* **5** 1-10
- [21] Mohapatra P, Deb S, Singh B, Vasa P and Dhar S 2016 Strictly monolayer large continuous MoS₂ films on diverse substrates and their luminescence properties *Applied Physics Letters* **108** 042101
- [22] Zhu D, Shu H, Jiang F, Lv D, Asokan V, Omar O, Yuan J, Zhang Z and Jin C 2017 Capture the growth kinetics of CVD growth of two-dimensional MoS₂ *npj 2D Materials and Applications* **1** 1-8
- [23] Zhou D, Shu H, Hu C, Jiang L, Liang P and Chen X 2018 Unveiling the growth mechanism of MoS₂ with chemical vapor deposition: from two-dimensional planar nucleation to self-seeding nucleation *Crystal Growth & Design* **18** 1012-9
- [24] Singh A, Moun M and Singh R 2019 Effect of different precursors on CVD growth of molybdenum disulfide *Journal of Alloys and Compounds* **782** 772-9
- [25] Zhu Z, Zhan S, Zhang J, Jiang G, Yi M and Wen J 2019 Influence of growth temperature on MoS₂ synthesis by chemical vapor deposition *Materials Research Express* **6** 095011

- [26] Feng S, Tan J, Zhao S, Zhang S, Khan U, Tang L, Zou X, Lin J, Cheng H M and Liu B 2020 Synthesis of Ultrahigh-Quality Monolayer Molybdenum Disulfide through In Situ Defect Healing with Thiol Molecules *Small* **16** 2003357
- [27] Ahn C, Park Y, Shin S, Ahn J-G, Song I, An Y, Jung J, Kim C S, Kim J H and Bang J 2021 Growth of Monolayer and Multilayer MoS₂ Films by Selection of Growth Mode: Two Pathways via Chemisorption and Physisorption of an Inorganic Molecular Precursor *ACS Applied Materials & Interfaces* **13** 6805-12
- [28] Yazyev O V and Louie S G 2010 Electronic transport in polycrystalline graphene *Nature materials* **9** 806-9
- [29] Ganorkar S, Kim J, Kim Y H and Kim S-I Effect of Precursor on Growth of MoS₂ Monolayer and Multilayer
- [30] Xie Y, Wang Z, Zhan Y, Zhang P, Wu R, Jiang T, Wu S, Wang H, Zhao Y and Nan T 2017 Controllable growth of monolayer MoS₂ by chemical vapor deposition via close MoO₂ precursor for electrical and optical applications *Nanotechnology* **28** 084001
- [31] Tao L, Chen K, Chen Z, Chen W, Gui X, Chen H, Li X and Xu J-B 2017 Centimeter-scale CVD growth of highly crystalline single-layer MoS₂ film with spatial homogeneity and the visualization of grain boundaries *ACS applied materials & interfaces* **9** 12073-81
- [32] Han G H, Kybert N J, Naylor C H, Lee B S, Ping J, Park J H, Kang J, Lee S Y, Lee Y H and Agarwal R 2015 Seeded growth of highly crystalline molybdenum disulfide monolayers at controlled locations *Nature communications* **6** 1-6
- [33] Lee C, Yan H, Brus L E, Heinz T F, Hone J and Ryu S 2010 Anomalous lattice vibrations of single-and few-layer MoS₂ *ACS nano* **4** 2695-700
- [34] Mignuzzi S, Pollard A J, Bonini N, Brennan B, Gilmore I S, Pimenta M A, Richards D and Roy D 2015 Effect of disorder on Raman scattering of single-layer MoS₂ *Physical Review B* **91** 195411
- [35] Coehoorn R, Haas C and De Groot R 1987 Electronic structure of MoSe₂, MoS₂, and WSe₂. II. The nature of the optical band gaps *Physical Review B* **35** 6203
- [36] Coehoorn R, Haas C, Dijkstra J, Flipse C d, De Groot R and Wold A 1987 Electronic structure of MoSe₂, MoS₂, and WSe₂. I. Band-structure calculations and photoelectron spectroscopy *Physical review B* **35** 6195
- [37] Dumcenco D, Ovchinnikov D, Marinov K, Lazic P, Gibertini M, Marzari N, Sanchez O L, Kung Y-C, Krasnozhan D and Chen M-W 2015 Large-area epitaxial monolayer MoS₂ *ACS nano* **9** 4611-20
- [38] Ohring M 2001 *Materials science of thin films*: Elsevier

- [39] Najmaei S, Liu Z, Zhou W, Zou X, Shi G, Lei S, Yakobson B I, Idrobo J-C, Ajayan P M and Lou J 2013 Vapour phase growth and grain boundary structure of molybdenum disulphide atomic layers *Nature materials* **12** 754-9
- [40] Wang W, Zeng X, Wu S, Zeng Y, Hu Y, Ding J and Xu S 2017 Effect of Mo concentration on shape and size of monolayer MoS₂ crystals by chemical vapor deposition *Journal of Physics D: Applied Physics* **50** 395501
- [41] Molina-Sanchez A and Wirtz L 2011 Phonons in single-layer and few-layer MoS₂ and WS₂ *Physical Review B* **84** 155413
- [42] Mak K F, He K, Lee C, Lee G H, Hone J, Heinz T F and Shan J 2013 Tightly bound trions in monolayer MoS₂ *Nature materials* **12** 207-11
- [43] Scheuschner N, Ochedowski O, Kaulitz A-M, Gillen R, Schleberger M and Maultzsch J 2014 Photoluminescence of freestanding single-and few-layer MoS₂ *Physical Review B* **89** 125406
- [44] Withanage S S and Khondaker S I 2019 CVD Growth of Monolayer MoS₂ on Sapphire Substrates by using MoO₃ Thin Films as a Precursor for Co-Evaporation *MRS Advances* **4** 587-92
- [45] Senthilkumar V, Tam L C, Kim Y S, Sim Y, Seong M-J and Jang J 2014 Direct vapor phase growth process and robust photoluminescence properties of large area MoS₂ layers *Nano research* **7** 1759-68

Supplementary information

Kinetics and Parameters of Epitaxial Monolayered Continuous large area Molybdenum disulfide Growth

Rakesh K. Prasad¹, Dilip K. Singh^{1*}

¹Birla Institute of Technology Mesra, Ranchi -835215 (India)

*Email: dilipsinghnano1@gmail.com

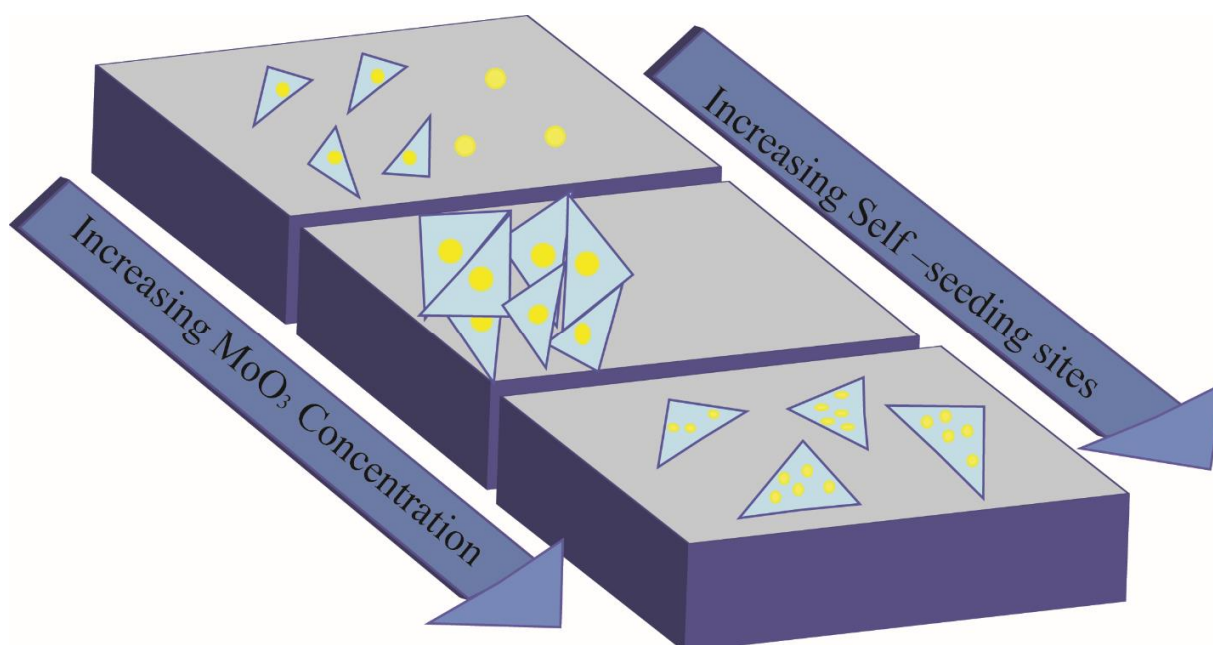


Fig. S1: Schematic diagram, illustrate the effect of concentration of MoO₃ precursor on self - seeding sites

Figure S1 schematically shows that lower concentration of MoO₃ helps to grown smaller crystal size of MoS₂ flakes with single seeding sites and with moderate amount of MoO₃. During growth, keeping other parameter constant like sulfur, gas flow rate and position of substrate

helps to grow large crystal size. Higher amount of MoO_3 concentration increases the density of self-seeding sites inside the single flakes which is further responsible for multi-layer growth.

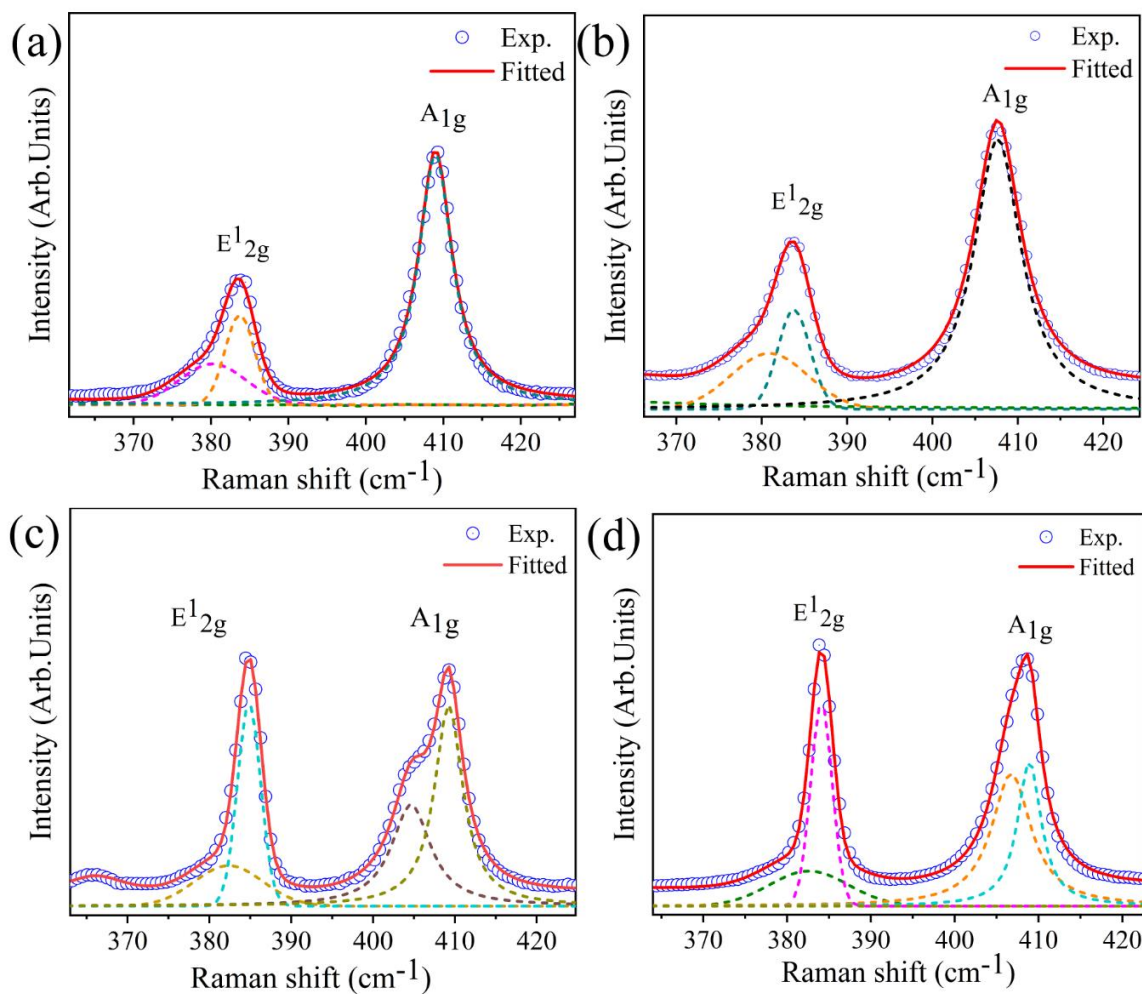


Fig. S2: Raman spectra plot for MoS_2 flakes grown under different concentration of MoO_3 (a) 10 mg (b) 20 mg (c) 25 mg (d) 30 mg

Fig. S2 shows fitted Raman spectra of grown MoS_2 sample with varying concentration of MoO_3 keeping other parameters constant. With lower concentration of MoO_3 (10 mg and 20 mg), A_{1g} shows single peak, but with higher concentration of MoO_3 (25 mg and 30 mg), A_{1g} peak requires two peaks to fit indicating incomplete formation of multilayer on monolayer MoS_2 .

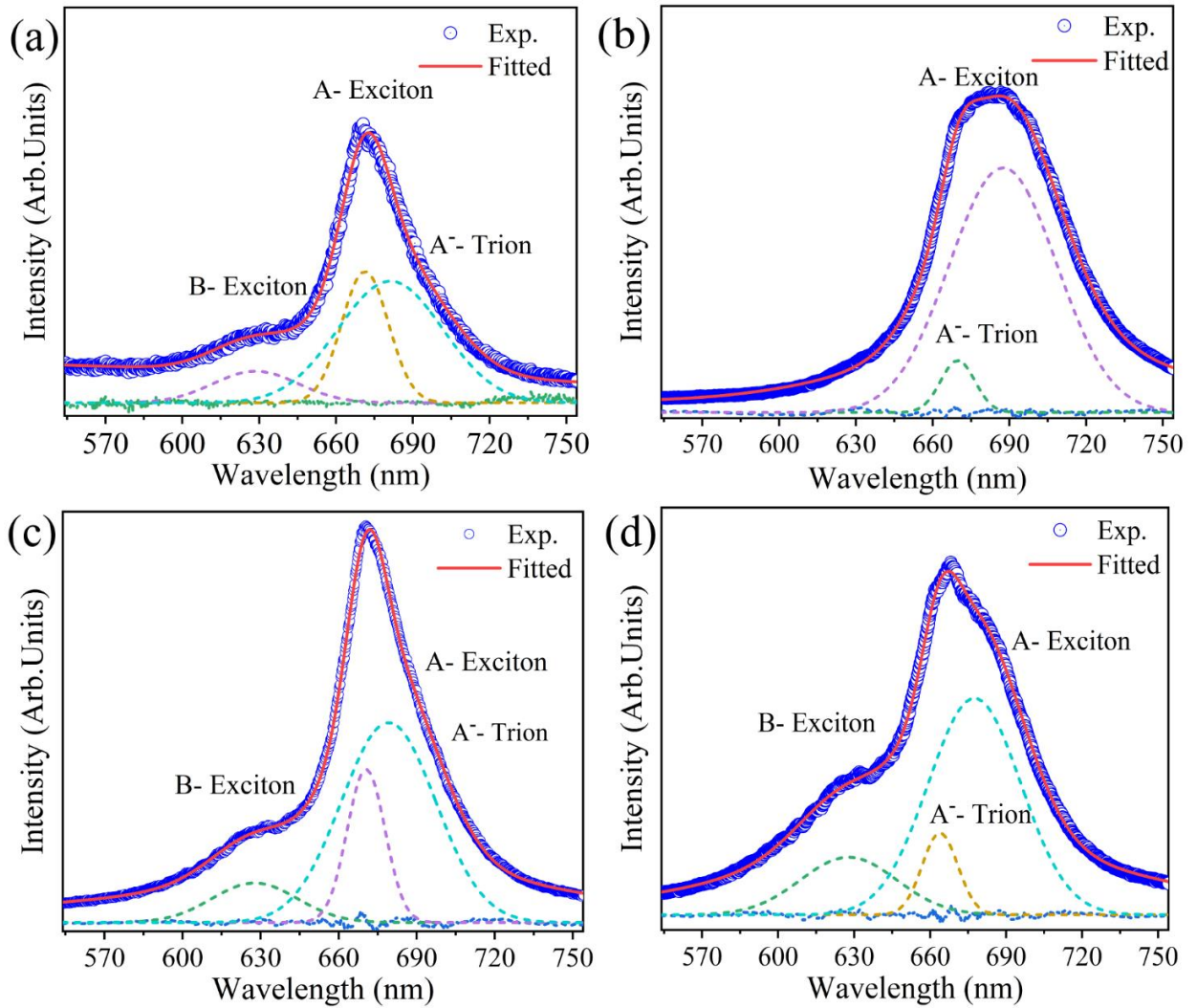


Fig. S3: Photoluminescence spectra plot for MoS₂ flakes grown under different concentration of MoO₃ (a) 10 mg (b) 20 mg (c) 25 mg (d) 30 mg

Fig. S3 show fitted photoluminescence spectra of MoS₂ grown by CVD using varying concentration of MoO₃. Three spectra line (A Exciton, A⁻-Trion and B- Exciton) are observed at ~ 627, ~ 670, and ~ 680 nm. 627 nm peak indicates B-Exciton 670 nm peak indicates A-Exciton and 680 nm peak indicates A⁻ -Trion, All peaks indicate high crystal quality of film growth of MoS₂ crystals.